MULTI–OBJECTIVE DESIGN OPTIMIZATION OF A MORPHING AILERON FOR A HYBRID ELECTRIC REGIONAL AIRCRAFT

Alessandro De Gaspari[1], Vittorio Cavalieri[1], Matteo Corti[1] & Sergio Ricci[1]

[1]Politecnico di Milano, Department of Aerospace Science and Technology, Via La Masa 34, 20156 Milano, Italy

Abstract

This paper describes the morphing aileron designed to be installed on the high aspect ratio wing of a hybrid–electric regional aircraft, in the framework of the Clean Aviation Joint Undertaking. The aim of this work is to replace the conventional hinged aileron with an innovative aileron characterized by a smooth continuous skin surface and able to reduce drag and actuation force compared to the traditional solution. The design phase is based on a multi–disciplinary design approach taking into account aerodynamic performances, kinematic and structural requirements, and actuation aspects, arriving at the design of a compliant structure able to achieve the external shapes that guarantee the performance requirements. The paper includes the description of the design levels and the results obtained. Moreover, numerical modelling and analysis of a full–scale demonstrator are reported, as well as a possible solution for the actuation system capable of achieving the desired structural behavior and the required bandwidth.

Keywords: aerodynamic performance, topology optimization, compliant structure, actuation mechanics, virtual prototype

1 Introduction

In the framework of the EU funded Hybrid Electric Regional Wing Integration Novel Green Technologies (HERWINGT) project, supported by the Clean Aviation Joint Undertaking, an innovative wing suitable for the future Hybrid Electric Regional Aircraft (HERA) is currently being designed to mitigate the environmental impact of air transportation, in accordance with the Europe's vision for sustainable aviation [1]. This wing design will benefit from all the technologies matured during the project, aimed at improving aerodynamic efficiency and developing light–weight wing structures and hybrid–electric propulsion.

One of the technologies being investigated is the morphing concept, which has the potential to increase the aerodynamic efficiency, reduce pollutant emissions and noise [2], and improve the structural efficiency. The role of Politecnico di Milano (Polimi) within the project is related to the design optimization of two different morphing devices:

- a full–scale, large–bandwidth morphing aileron able to replace the traditional hinged aileron;

- a morphing droop nose for high–lift conditions, working in combination with a morphing flap.

This paper describes the development of the morphing aileron to be installed on the innovative wing. From the aerodynamic point of view, it is well known that the smooth shape change provided by morphing devices enables improved efficiency [3], minimizing aerodynamic drag during maneuvers. However, the morphing concept is a viable option if there is an overall advantage [4], i.e. if the aerodynamic benefit is achieved in combination with a weight benefit. In the case of an aileron, a large part of the weight comes from the actuation system. Thanks to the greater design freedom of morphing devices, the morphing aileron presented in this paper is able to minimize the aerodynamic drag and, at the same time, the maximum actuation force, which determines the choice of the actuation system.

Moreover, reducing the actuation force also means a smaller actuator, suitable to be installed inside the wing which has been designed to increase the aspect ratio as much as possible to minimize the induced drag.

The design specification of the work described here is to replace the traditional hinged aileron with a morphing aileron able to guarantee the lift variations produced by the conventional solution, in different flight conditions, considering a maximum rigid rotation of ± 30 deg, minimizing at the same time the aerodynamic drag and the total actuation force. The initial requirements for the wing include a rear spar located at 60% of the local chord. In accordance with this information, the hinge position of the traditional aileron and the chordwise position where the morphing control surface begins to deform have been placed at 70% of the local chord, in order to have space for the positioning of the actuator, which should preferably be located outside the wing–box. The initial requirements in terms of lift variation are computed using SU2 by means of 2D Reynolds–averaged Navier–Stokes (RANS) simulations [5]. The maximum deflections of hinged and morphing ailerons are evaluated and compared at the design maneuvering speed, characterized by Mach = 0.29 and zero altitude. The airfoil at the aileron root is used for the aerodynamic computations. The aerodynamic results in terms of momentum in the chord direction for the downward and upward rigid rotations are depicted in Figure 1. It can be seen that these solutions are characterized by large separation regions. It is expected that this situation can be improved thanks to the smooth curvature variation provided by the morphing aileron.
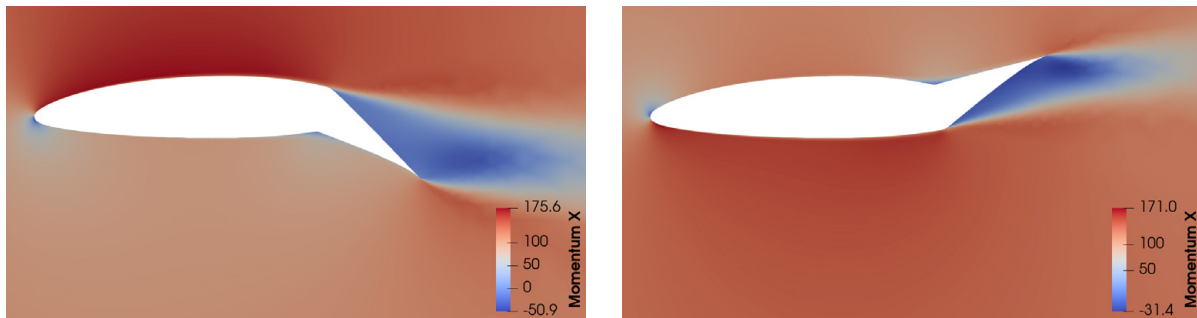
Figure 1 – Contour of the momentum in the chord direction for the traditional hinged aileron.

The morphing aileron deflection is enabled by the skin deformation, while the actuation system must be connected to the lower skin, which is free to slide along the wing surface. The sliding of the lower skin in both directions allows downward and upward morphing shapes to be achieved [6].

The optimal design of the morphing aileron has been performed via a multi–level approach based on the compliant structure concept. In the first level, which is described in Section 2, an aero–structural shape optimization works to define optimal morphing shapes taking into account aerodynamic, structural and actuation aspects. In the second level, which is described in Section 3, a dedicated topology and sizing multi–objective optimization tool is used to define the optimal internal structure able to deform itself for matching, once actuated, all optimal shapes coming out from the first level [7, 8]. After the topological synthesis, the designed solution is used for the realization of a complete finite element model (FEM) of a two-meter span aileron, as described in Section 4. In this work, the aerodynamic and structural design phases of the morphing compliant device are independent on the choice of the actuation system, but at the end a suitable selection of the actuator and the design of a dedicated kinematic chain are essential to implement the designed solution, as described in Section 4.2.

2   Design Optimization of the Aerodynamic Morphing Shapes

The aero–structural shape optimization consists of a two–objective shape optimization defining the most efficient shapes able to:

1. minimize the aerodynamic drag in the morphing configuration;

2. minimize the force to be applied to the lower skin to produce the shape changes due to the morphing,

subject to aerodynamic and structural constraints. The aerodynamic constraint accounts for the same lift variation introduced by the rotation of the traditional hinged aileron. The structural constraint allows the structural limits of the morphing skin to be taken into account. The optimization scheme consists of two nested optimization loops: the inner one produces only feasible morphing shapes that satisfy the structural constraints, while the outer one performs the aerodynamic evaluation. In this way, only morphing shapes that satisfy all structural and mechanical constraints are considered in the aerodynamic computation.

The shape optimization is coupled with a parameterization method, called Class/Shape function Transformation (CST) technique, which was extended so that shape perturbations due to the morphing could be introduced in a feasible way. The parameterization method can reproduce the structural behavior of the morphing skin in an analytical way, so without the need of finite element analyses [9]. In this study, the aileron shape changes due to the morphing were parameterized using two design variables: the trailing–edge equivalent rotation δ_{TE} and the airfoil boat–tail angle variation $\Delta\beta$.

The CST method is then coupled with an aerodynamic solver and a mathematical method which can be used to estimate the actuation energy or the force required to deploy the morphing aileron. On the one hand, lift and drag coefficients, as well as the pressure distribution over the wing, are computed by RANS computations. On the other hand, the total actuation energy can be calculated by knowing the strain energy required to deform the morphing skin and the aerodynamic work required to counteract the aerodynamic forces [6, 10].

The total actuation energy is valid for any actuator installed inside the morphing device, while the actuation force depends on the actuation system. At this stage, the considered force is the force that applied to the lower skin, tangential to the airfoil lower surface at 70% of the chord, is able to provide the sliding displacement required to achieve the target morphing shapes. The displacement values, for the downward and upward deflections, can be easily computed with the CST because they correspond to how much the lower skin becomes shorter or longer, respectively. Therefore, the actuation force can be minimized by looking for a morphing shape which minimizes the total energy or maximizes the sliding displacement of the skin.

The shape optimization problem is solved by using a Design of Experiments (DOE) approach based on the response surface method (RSM). Surrogate models of the objective and constraints functions are built using a Radial Basis Function (RBF) interpolation. The outputs of interest are computed for a Latin hypercube sample in the space of the design variables. The results obtained are used to construct the response surfaces of interest, i.e. lift coefficient, drag coefficient, strain distribution along the skin and actuation force.

Since the two–objective shape optimization finds multiple optimal solutions, at the end of the process the optimal shape solution can be selected from the Pareto front. The procedure was repeated to find shapes corresponding to downward and upward deflections. The Pareto fronts depicted in Figure 2 show how the drag coefficient and the actuation force are conflicting requirements. Three different solutions are highlighted, corresponding to different values of the shape design variables. The selected morphing shapes correspond to the red circles. The selection was made with force minimization as the main design criterion. However, these shapes represent Pareto points so they also minimize drag. Indeed, the polar curves reported in Figure 3 show the aerodynamic benefit of the morphing aileron compared with the conventional hinged aileron. The morphing solutions are characterized by less drag to achieve the same lift variations provided by the hinged solutions. In addition, while the upward hinged aileron stalls for angles of attack less than -2 deg, the corresponding morphing solution delays the stall by 4 deg making it much more gradual.

The aerodynamic properties of the selected optimal morphing shapes are also shown in Figure 4 in terms of contours of aerodynamic momentum for both the downward and upward deflections. These results, compared with those in Figure 1, show how morphing avoids, or at least greatly reduces, flow separation and boundary layer detachment.

The CST technique enables the computation of the skin sliding displacement which is equal to -45 mm and 49 mm for the downward and upward morphing deflections, respectively, at the root section of the aileron. The corresponding values at the tip section of the aileron are -31 mm and 33 mm.

The optimal shape variations obtained during this phase are propagated along the wingspan, in the
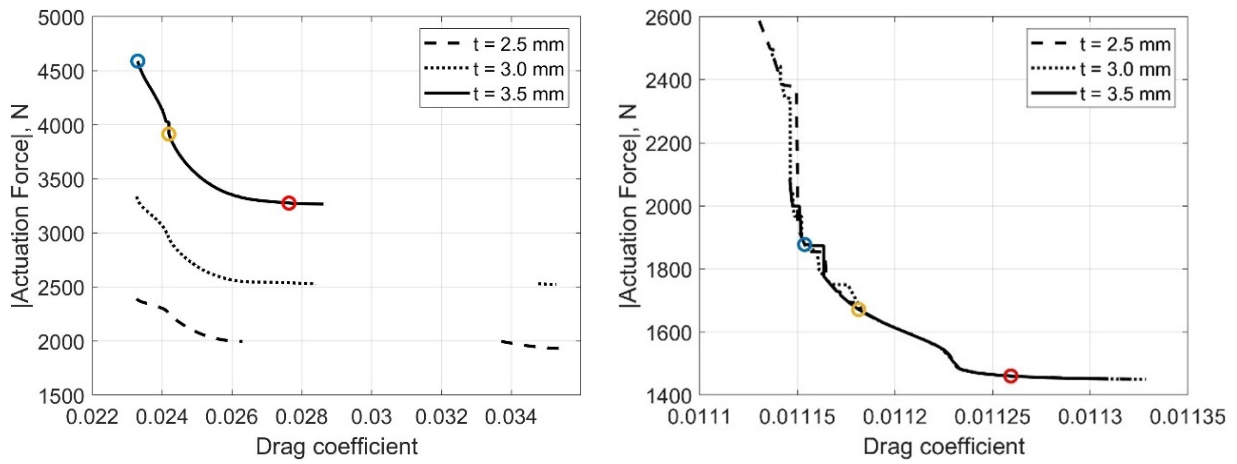
Figure 2 – Pareto fronts obtained by the shape optimization for the downward (left) and upward (right) deflection cases, for different values of skin thickness t.
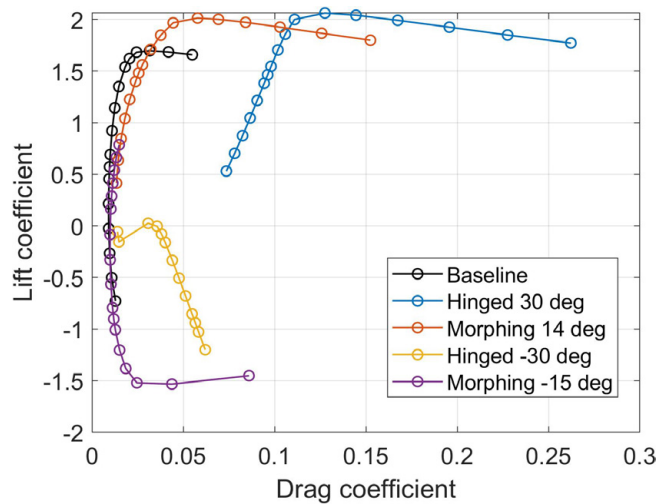
Figure 3 – Comparison between morphing and hinged aileron in terms of aerodynamic polar curves.

whole aileron region, obtaining the CST models of the 3D morphing shapes, which are shown in Figure 5.

These shapes and information are then used as targets for the design of the internal compliant structure of the morphing aileron, a structure capable, once actuated, of deforming as established by shape optimization. The structural design can be repeated for different sections along the span. A solution for the aileron root section has been presented in [11]. The remainder of this paper focuses on a solution developed for the aileron demonstrator that will be tested in the Polimi's Wind Tunnel facility, by the end of 2025.

The aircraft wing is a strut-braced wing equipped with aileron devices of five meters span. Due to constraints related to the experimental facility, the demonstrator of the device is limited to the outer two meters of span. Figure 6 depicts the complete wing and a demonstrator of the structural wing–box equipped with the morphing aileron demonstrator that is described in the following sections.
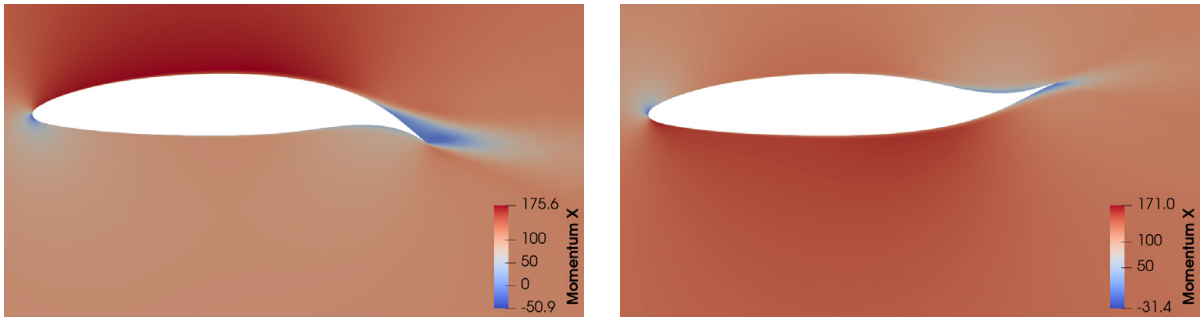
Figure 4 – Contour of the momentum in the chord direction for the morphing aileron.
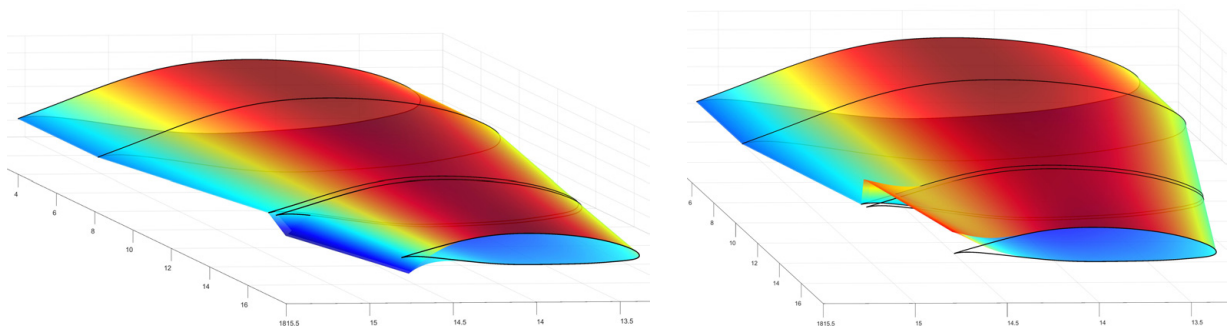
Figure 5 – 3D CST models of the optimal downward and upward deflections of the morphing aileron installed on the reference wing.
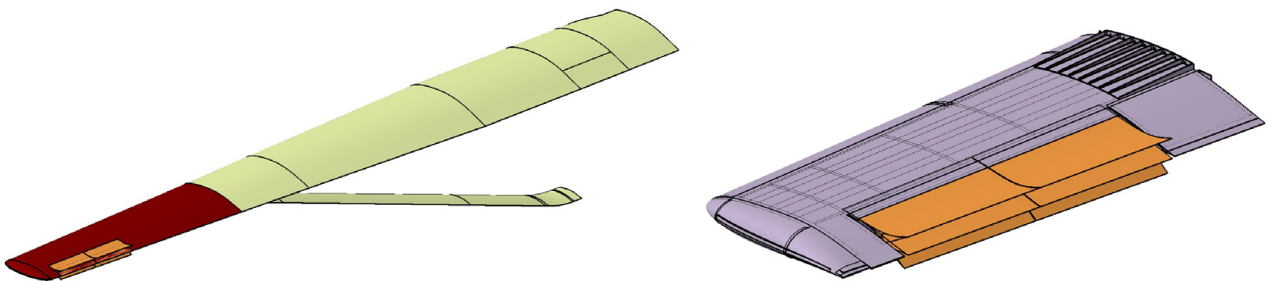
Figure 6 – Aircraft wing (left) and structural wing–box demonstrator equipped with the morphing aileron (right).

3 Optimum Structural Design

The structural design of the morphing aileron is based on the distributed compliance concept and uses an in–house design tool to obtain a compliant structure made of flexible elements, rather than rigid mechanical components. This optimization tool is based on a multi–objective Genetic Algorithm (GA) coupled with non–linear finite element analyses. The optimization algorithm uses dedicated crossover and mutation functions that allow topology, size and shape design variables to be combined in the same optimization process.

Different objective functions are considered in the optimization:

1. kinematic requirement to achieve the optimal downward deflection when the lower skin is pulled;

2. kinematic requirement to achieve the optimal upward deflection when the lower skin is pushed;

3. structural requirement to keep the aileron in its undeformed shape when it is not actuated;

4. minimization of the actuation force in all cases (optional),

under material constraints and dynamic requirements to guarantee a behavior compatible with the servo–controller bandwidth. The sliding displacement values of the skin for the downward and upward morphing deflections come from the results of the shape optimization. These values are used to perform imposed–displacements non–linear finite element analyses during the execution of the GA, while the actuation forces are calculated as constraint forces in the lower skin points where the displacement is imposed. The design optimization is performed for the aileron section located at two meters from tip, since this section represents the root of the aileron demonstrator. Aerodynamic loads at the maneuvering speed are considered for the kinematic requirements, whereas the aerodynamic loads at the dive speed are considered for the structural requirement.

Since the multi–objective GA finds multiple optimal solutions, the optimal structural solution can be selected from the Pareto front, taking into account manufacturing requirements which are not included in the optimization problem.

A solution was selected on the Pareto front and the corresponding structural configuration is shown in Figure 7, in terms of 3D deformations related to both the downward and upward deflection, together with the contour of the maximum principal strains. The designed solution consists of a flexible skin,
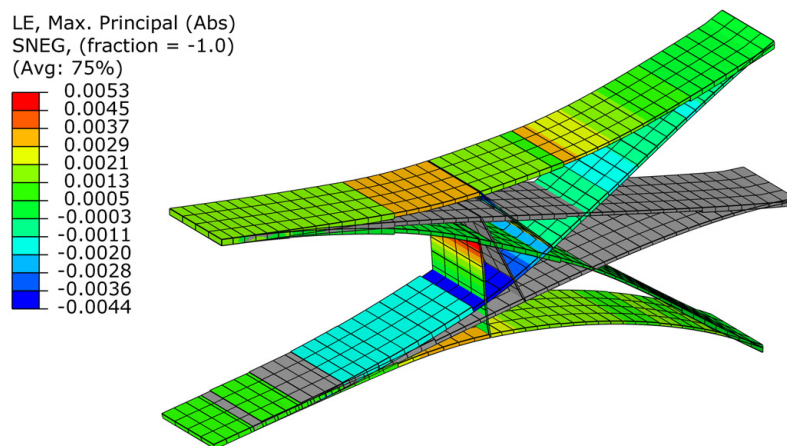
Figure 7 – Finite element model of the optimum structural solution of morphing aileron from topology optimization and results obtained when the model is actuated to achieve its maximum upward and downward deflections.

characterized by variable thickness in the chordwise direction, and a compliant spar, both in glass-fiber material. The strain values satisfy the material limits and are compatible with the estimate obtained from the CST technique during the shape optimization.

The designed morphing solution is compared with the corresponding hinged solution, in terms of overall aerodynamic benefit and actuation force. The actuation force required for the morphing

aileron consists of a structural contribution to perform the morphing process and an aerodynamic contribution to counteract the external aerodynamic loads. The total actuation forces required for the morphing aileron are obtained from the finite element analyses performed on the designed solution. The actuation force for the hinged aileron is entirely due to aerodynamic loads. This force is estimated from the hinge moment calculated on the rigidly rotated aileron, assuming an internal leverage. The comparison between conventional hinged aileron and the designed morphing aileron at the maximum deflections is reported in Figure 8, in terms of drag coefficient and actuation force, at the maneuvering speed for a 0 deg angle of attack. The actuation forces are related to a span of
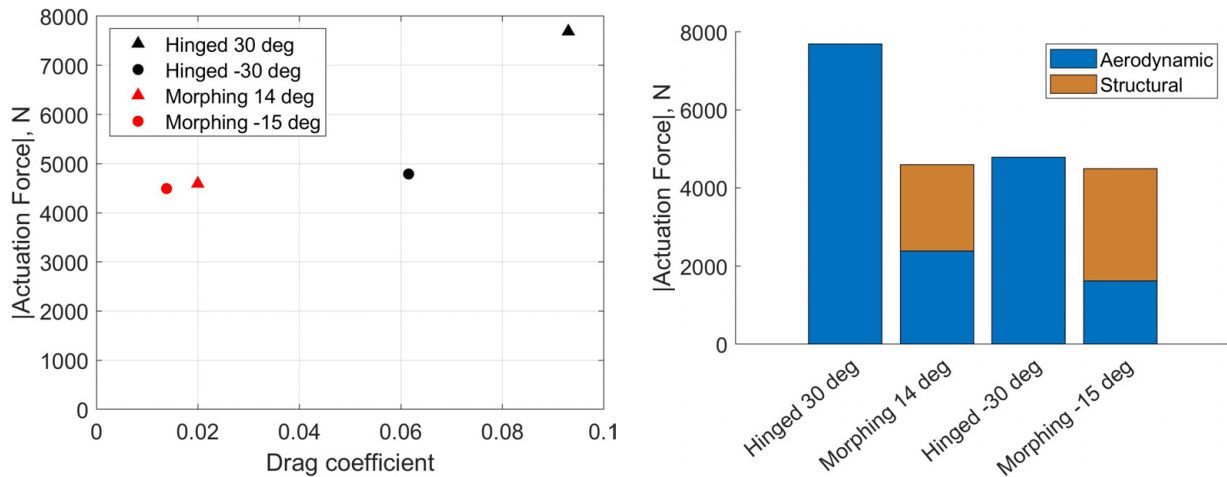
Figure 8 – Comparison of aerodynamic and actuation performances between hinged and morphing aileron (left). Aerodynamic and structural contributions to the actuation forces (right).

one meter and are given in absolute value. However, it is important to remember that downward and upward deflections require opposite sign for the force, corresponding to pulling and pushing of the lower skin, respectively.

It is evident how, although the morphing solution pays a component of force due to the energy required to deform the structure, its total actuation force is much lower than that required to rotate the traditional hinged aileron. This is due to the low value of mechanical work required to counteract external aerodynamic forces in the case of the morphing aileron. Therefore, the design phase has been successful in achieving a morphing aileron that, thanks to the multiple degrees of freedom involved in the shape change, has been optimized to improve both aerodynamic performance and the force required to deploy it.

Having demonstrated the potential benefits associated with the morphing solution, the work done within the project continues with the development of a full–scale prototype, for the experimental validation of the proposed concept, in terms of aerodynamic, structural, and dynamic properties of the morphing device. The conceived demonstrator is full–scale in chord, but it has a limited spanwise extension of two meters, to be tested in the Polimi's Wind Tunnel. Moreover, considering a maximum Mach number of 0.15 in the wind tunnel facility, lower than the design conditions adopted for the real aircraft, a sizing modification is applied for the experimental demonstrator. This modification, which does not affect the quality of the external morphing shape, is adopted to avoid oversizing the actuation system with respect to the actual requirements for the planned wind tunnel test campaign. By applying a thickness reduction of 27% to the entire compliant structure, the morphing shape change capability is preserved in accordance with the target. The comparison between deformed and target shapes at the root section of the demonstrator is represented in Figure 9.
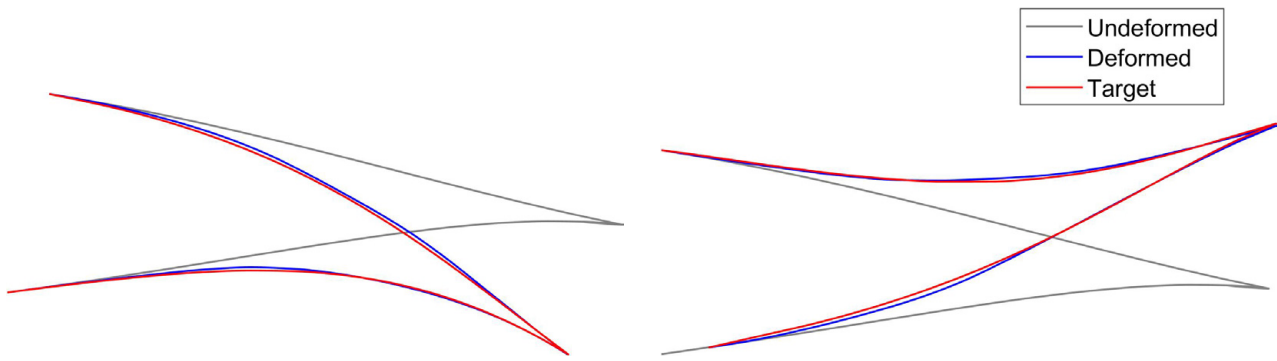
Figure 9 – Comparison between deformed and target shapes for the downward (left) and upward (right) deflections.

4   Demonstrator Virtual Model

The optimal structural configuration obtained in the previous section is the starting point for the realization of a virtual model of the complete demonstrator. Actually, the two-meter aileron demonstrator will be realized in two separate devices. Therefore, there will be two devices, each having one meter of span and a dedicated actuation system, resulting in two devices that can be independently actuated during the experimental test. The finite element model of the complete demonstrator is realized in Abaqus and it is depicted in Figure 10. It is made of shell elements both for the skin and the internal flexible spar. The model is clamped on the upper skin at 70% of the chord, representing the connection with the non-morphing part of the wing. The lower skin at 70% of the chord, which must be free to slide, is not constrained with exceptions in correspondence of four actuation input points, two for each device. At these points, enforced-motion boundary conditions are imposed, using displacement values compatible with the CST computations. In particular, these values are obtained for the airfoils at the two extreme sections, and then they are computed at the required spanwise locations by linear interpolation along the span. The motion imposed at these points is transmitted to the skin by means of Abaqus distributing coupling constraints, where the nodes of the skin are made dependent on the translation and rotation of the reference node represented by the input point. A reinforcement on the lower skin guarantees the sufficient stiffness in the spanwise direction, to sustain the aerodynamic loads. In the modelling phase of the described FEM, no more details of the actuation system are included, but a dedicated design of the actuation mechanism, discussed in Section 4.2, is required to guarantee the achievement of the assumed displacements for the actuation input points on the skin.
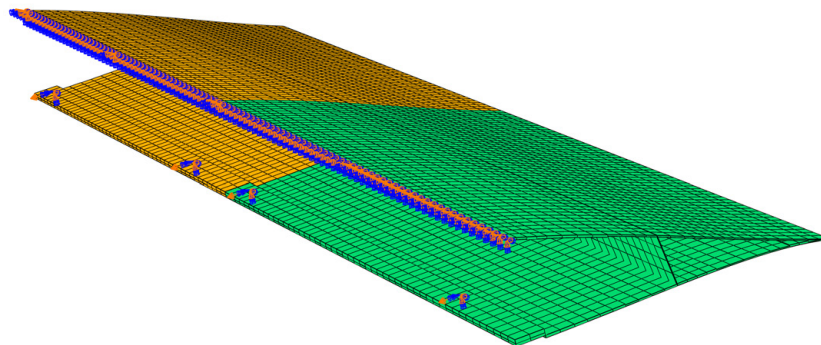
Figure 10 – Finite element model of the complete morphing aileron demonstrator.

4.1   Structural and Shape Assessment

The described FEM is used to verify the 3D behavior of the device in terms of structural feasibility and shape quality assessment. Nonlinear finite element analyses with enforced motion at the actuation input points are performed, also considering the application of pressure loads on the external surface.

The downward and upward deflected configurations are analyzed, and the results obtained for the two extreme deflections are overlapped in Figure 11, which also depicts the maximum principal strains in the deformed structure. Considering that the maximum allowable strain for a glass-fiber fabric exceeds 1%, the structural feasibility is assessed.
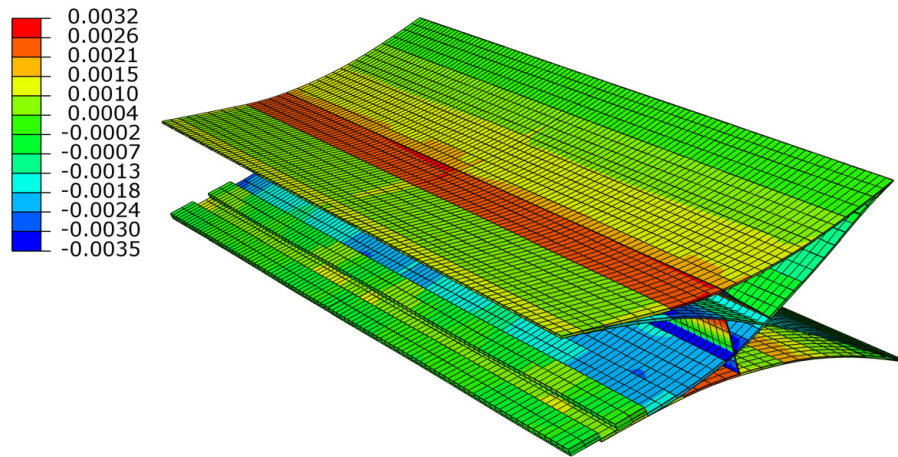
Figure 11 – Finite element results in terms of maximum principal strains for the complete morphing aileron demonstrator, for downward and upward maximum deflections.

Having enforced the motion of the input points, the reaction forces measured at these points are the data required for the mechanical design of the kinematic chain and the selection of a commercial off-the-shelf (COTS) actuator, as established in the initial requirements of the project.

Concerning the shape quality assessment, the achieved deformed surfaces are very smooth and they exhibit limited discrepancies compared to the target shapes determined in the first design level. The comparison between FEM deformed and target shapes is reported in Figure 12. Moreover, it
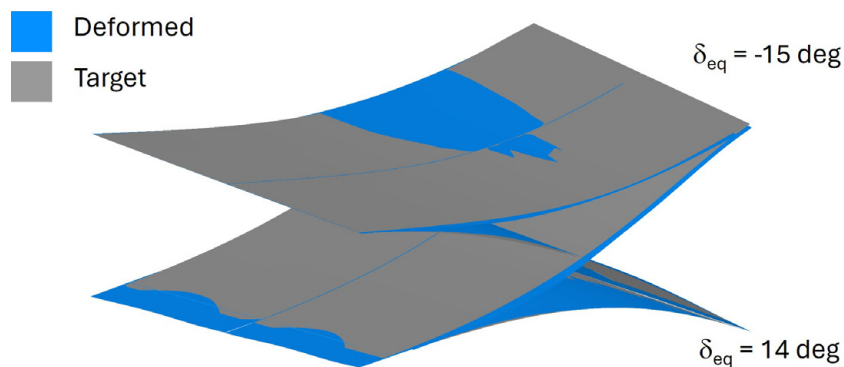
Figure 12 – Comparison between 3D deformed shapes and target shapes.

is assessed that the sensitivity of external shape to the application of the aerodynamic loads is very limited.

Finally, a modal analysis is performed in the configuration with fixed actuation points. The first mode shape for each of the one-meter demonstrators is reported in Figure 13. The corresponding frequencies are 38.8 Hz and 39.7 Hz. These values are high enough to reasonably exclude a coupling with the required actuator bandwidth of 10 Hz. Further dynamic studies including modelling of the kinematic chain and the servo-control will be considered in future work in preparation for the structural dynamic tests planned after the manufacturing of the first prototype. The proximity of the first frequencies of the two demonstrators is the result of the final design refinement, aimed at achieving two aileron devices characterized by the same equivalent stiffness, denoted here as the ratio between the actuation force at the input point and the corresponding sliding displacement. This is achieved by reducing the thickness values of the outer device by 8% with respect to the inner one.
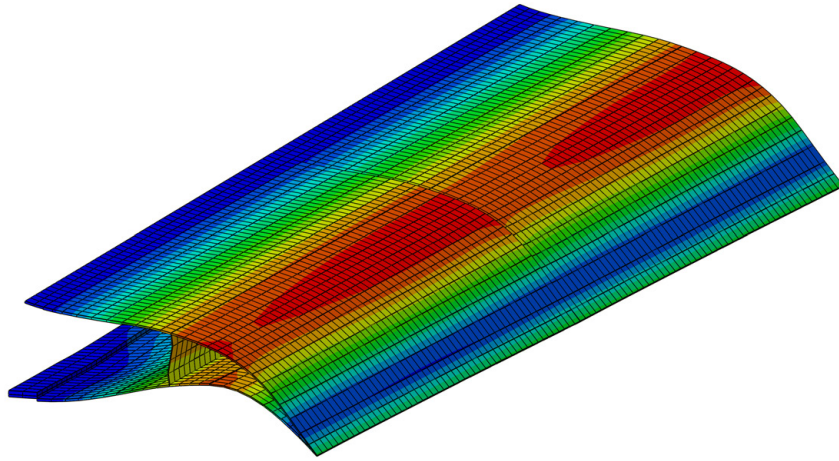
Figure 13 – First mode shapes for the demonstrators.

4.2 Actuation System

Due to the space limitations, related to the rear spar position at 60% of the chord, given the bandwidth and the force requirements for the actuation of the aileron, it is not feasible to locate the motor parallel to the actuation direction of the skin. This would be the simplest solution for actuating the skin, but this is not possible with the electric motor technology available for industrial applications. Therefore, the motor must be mounted parallel to the rear spar, and a linkage is required to transmit the motion to the actuation point.

A linear actuator is selected and it is connected to a Scott Russell linkage. Thanks to the limited number of components, the mass of the mechanism between the motor and the compliant structure is kept to a minimum, and this is beneficial to not decrease the dynamic performance of the solution. Figure 14 shows a schematic representation of the Scott Russell linkage. The motor should be connected to point A and actuates linearly in the x direction. The horizontal displacement Δx_A of point A is transformed into a vertical displacement Δy_C of point C, which will be connected to the lower skin. The relationship between these two displacements is:

$$\Delta y_C = \sqrt{4L_1^2 - (2L_1 cos\theta_0 + \Delta x_A)^2} - 2L_1 sin\theta_0 \tag{1}$$

where θ_0 is the angle between rod 2 and the shaft axis direction in the neutral position of the linkage, i.e. when the morphing aileron is in the undeformed configuration. The nonlinearity of the relation is depicted in Figure 15, which also shows the relationship between angle θ and displacement Δx_A.

A single motor can be connected to several Scott Russell linkages, that would be attached to different spanwise positions of the aileron. In the proposed solution, a single motor and two mechanisms are adopted for each one-meter device. This solution is illustrated in Figure 16. A dedicated design of the linkage, in terms of length of the rods and angle in the neutral position, is required to minimize the actuation force, taking into account the available space. In Figure 17 it is possible to see how the chordwise movement introduced by the Scott Russell mechanism is oriented in such a way to be parallel to the lower skin.

In general, the proposed kinematics can be adopted to limit the number of actuators, which could be located closer to the wing root, to minimize the inertia of the solution. Another advantage of this linkage is its ability to resist undesired lateral loads that would be absorbed by the main bearings at point D. This renders this solution more robust to unexpected scenarios and protects the motor.

Regarding the transmission of forces, the relationship between the vertical force F in C, which represents the reaction of the deformed aileron, and the motor actuation force in A is:

$$F_{motor} = F_{skin}/\tan\theta, \tag{2}$$

and it is represented in Figure 18.
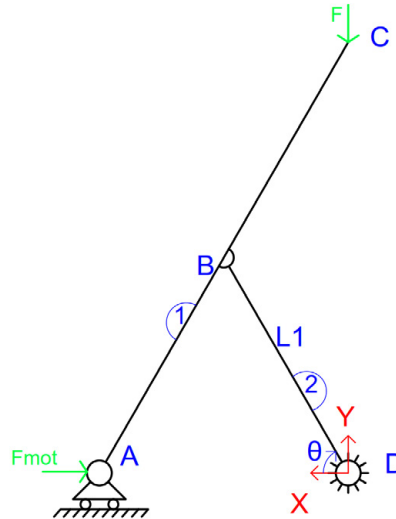
Figure 14 – Scott Russell linkage used to connect the actuator and the morphing device.
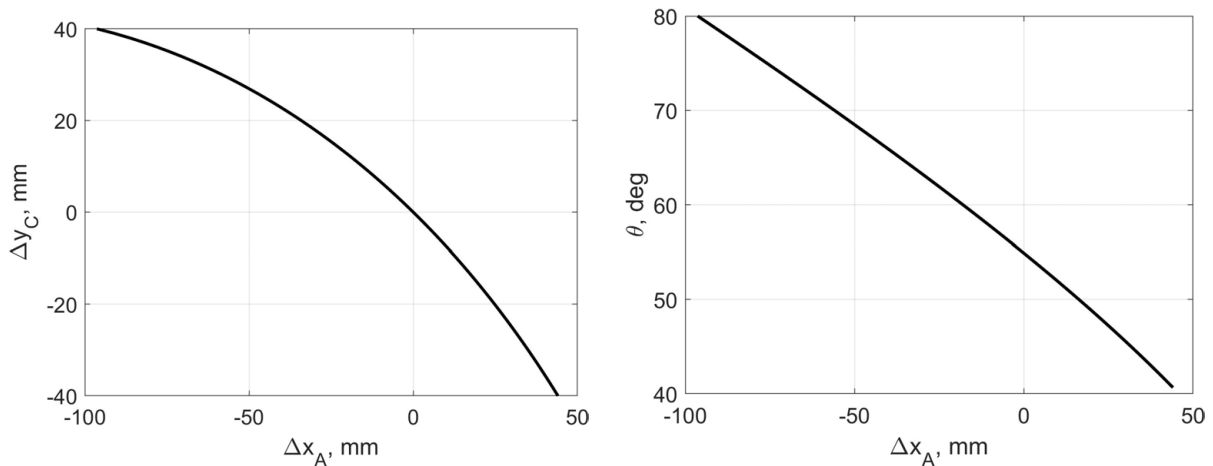
Figure 15 – Dependence of lower skin displacement (left) and rotation angle of the linkage (right) on the actuator stroke.

Regarding the selection of the motor, a geared motor is not suitable, due to the high bandwidth requirement. Only induction motors can provide the required actuation speed. However, this solution has drawbacks in terms of weight and temperature. These motors are usually heavier and generally larger. In addition, these motors must be water cooled as their performance is strictly temperature dependent. The need for a separate dedicated cooling solution can be a complication.

Regarding the weight penalty, it is not a major issue for the purpose of the test, since these motors will only be used for the wind tunnel tests, while they do not represent the full–scale actuation solution, which will be addressed by other partners within the project. With regard to the heating problem, it has been verified that the cooling system can be accommodated in the space available and it is sufficient to guarantee the required performance in terms of maximum forces.
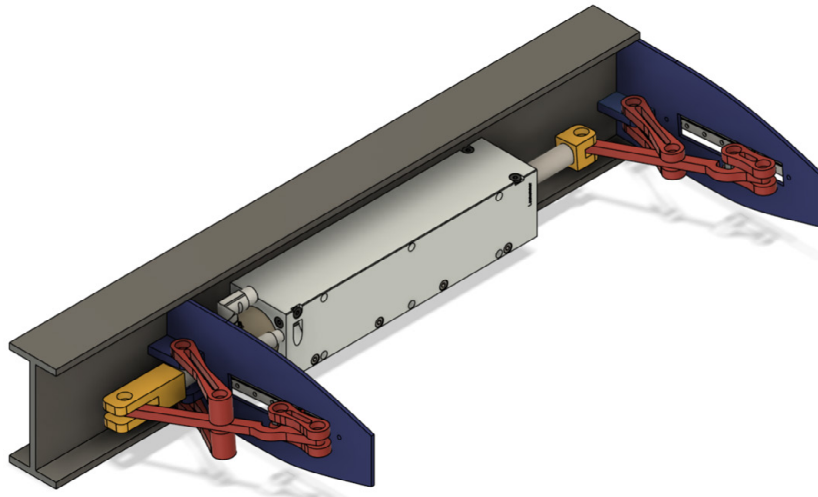
Figure 16 – Linear motor connected to two Scott Russell linkages for the actuation of the morphing aileron.
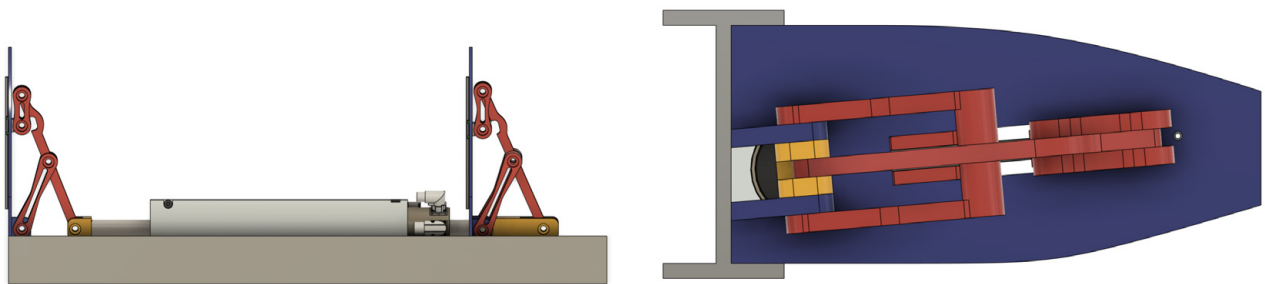
Figure 17 – Top and lateral views of the actuation mechanics.
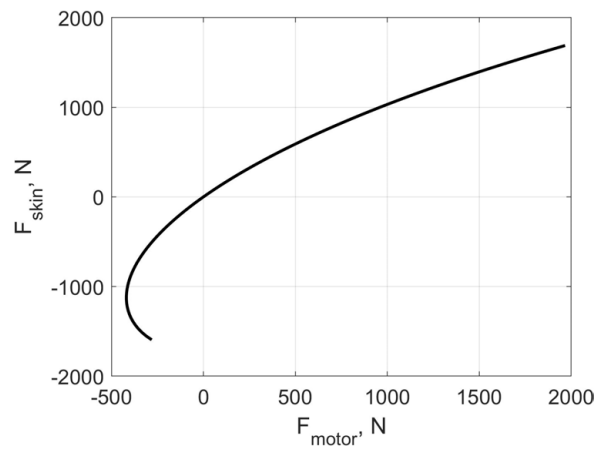
Figure 18 – Relationship between aileron reaction force on the linkage and motor actuation force.

5   Conclusion

This paper has described the design of a morphing aileron based on a multi–disciplinary optimization approach. Aerodynamic shape optimization has been performed to define optimal external shapes capable of achieving improved aerodynamic efficiency compared to a corresponding hinged aileron, while also reducing the required actuation force. Structural optimization has been carried out to realize a compliant structure capable of producing the defined target shapes. On the basis of the solution obtained, a virtual model of a real-scale demonstrator of the device has been realized for the assessment of the structural feasibility and the shape quality. Finally, the actuation system conceived to drive the morphing aileron has been presented. Future work will include dynamic and aeroelastic analyses of the virtual demonstrator in preparation for the ground and wind tunnel testing of the morphing aileron prototype.

Contact Author Email Address

mailto: alessandro.degaspari@polimi.it

Disclaimer

Funded by the European Union. Views and opinions expressed are however those of the author(s) only and do not necessarily reflect those of the European Union or Clean Aviation Joint Undertaking. Neither the European Union nor the granting authority can be held responsible for them.

References

[1] European Commission and Directorate-General for Research and Innovation. *Fly the Green Deal – Europe's vision for sustainable aviation*. Publications Office of the European Union. 2022. doi:10.2777/732726.

[2] Monner H, Kintscher M, Lorkowski T, and Storm S. Design of a smart droop nose as leading edge high lift system for transportation aircrafts. *50th AIAA/ASME/ASCE/AHS/ASC Structures, Structural Dynamics, and Materials Conference 17th AIAA/ASME/AHS Adaptive Structures Conference 11th AIAA No*. p. 2128. 2009. doi:10.2514/6.2009-2128.

[3] Woods B, Bilgen O, and Friswell M. Wind tunnel testing of the fish bone active camber morphing concept. *Journal of Intelligent Material Systems and Structures*. Vol. 25, No. 7, pp. 772–785. 2014. doi:10.1177/1045389X14521700.

[4] Weisshaar T. Morphing aircraft systems: historical perspectives and future challenges. *Journal of aircraft*. Vol. 50, No. 2, pp. 337–353. 2013. doi:10.2514/1.C031456.

[5] Palacios F, Alonso J, Duraisamy K, Colonno M, Hicken J, Aranake A, Campos A, Copeland S, Economon T, Lonkar A, Lukaczyk T, and Taylor T. Stanford University Unstructured (SU^2): An open–source integrated computational environment for multi–physics simulation and design. *51st AIAA Aerospace Sciences Meeting including the New Horizons Forum and Aerospace Exposition*. Grapevine, Texas. pp. 1 – 60. 5 January 2013. doi:10.2514/6.2013-287.

[6] De Gaspari A. Study on the actuation aspects for a morphing aileron using an energy–based design approach. *Actuators*. Vol. 11, No. 7. 2022. doi:10.3390/act11070185.

[7] De Gaspari A and Ricci S. A two–level approach for the optimal design of morphing wings based on compliant structures. *Journal of Intelligent Material Systems and Structures*. Vol. 22, No. 10, pp. 1091–1111. 2011. doi:10.1177/1045389X11409081.

[8] De Gaspari A. Multiobjective optimization for the aero-structural design of adaptive compliant wing devices. *Applied Sciences*. Vol. 10, No. 18, pp. 30. 2020. doi:10.3390/app10186380.

[9] De Gaspari A and Ricci S. Knowledge–based shape optimization of morphing wing for more efficient aircraft. *International Journal of Aerospace Engineering*. Vol. 2015, 325724, pp. 1 – 19. 2015. doi:10.1155/2015/325724.

[10] Bauchau O and Craig J. *Structural analysis: with applications to aerospace structures*. Solid Mechanics and Its Applications (SMIA, volume 163). Springer Science & Business Media. 2009. doi:10.1007/978-90-481-2516-6.

[11] Cavalieri V, De Gaspari A, and Ricci S. Aero-structural design optimization of a morphing aileron considering actuation aspects. *AIAA SCITECH 2024 Forum*. p. 2113. 2024. doi:10.2514/6.2024-2113.